ACS OMEGA

Article

Cite This: ACS Omega 2019, 4, 1995−2000

http://pubs.acs.org/journal/acsodf

Selective Adsorption of Water, Methanol, and Ethanol by Naphthalene Diimide-Based Coordination Polymers with Constructed Open Cu^{2+} Metal Sites and Separation of Ethanol/Acetonitrile

Guo-Bi Li,[†] Bai-Qiao Song,[‡] Shi-Qiang Wang,[‡] Ling-Min Pei,[§] Sheng-Gui Liu,[†] Jiang-Li Song,[†] and Qing-Yuan Yang*[,∥]

[†]School of Chemistry and Chemical Engineering, Lingnan Normal University, Zhanjiang 524048, People's Republic of China

[‡]Department of Chemical Sciences, Bernal Institute, University of Limerick, Limerick V94 T9PX, Republic of Ireland

[§]Department of Applied Chemistry, School of Science and [∥]School of Chemical Engineering and Technology, Xi'an Jiaotong University, Xi'an 710049, China

Supporting Information

ABSTRACT: The selective separation of ethanol/acetonitrile by porous materials has rarely been observed owing to their similar physicochemical properties. In this work, we report a new coordination network, $[Cu_2(4\text{-pmntd})_2(opd)_2]$(4-pmntd = *N*,*N*′-bis(4-pyridymethy)naphthalene diimide, opd = disodium 1,2-benzenedicarboxylate), which exhibits selective separation of ethanol over acetonitrile. The weak coordination bonds formed by unsaturated Cu^{2+} sites and hydroxyl groups are the key to such performance.

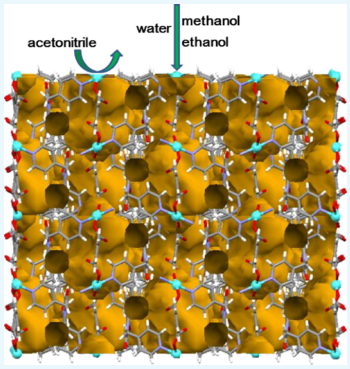

INTRODUCTION

Acetonitrile (CH_3CN) is an important organic solvent in the chemical industry, for example, acetonitrile is usually used in the manufacture of pharmaceuticals and photographic films.[1] Acetonitrile was also found to play an important role in the field of liquid chromatography because of its low viscosity and low chemical reactivity.[2,3] Catalytic dehydrogenation from ammonia and ethanol is generally used in acetonitrile production.[4] This method usually introduces some contaminants, such as unreacted ethanol. Thus, it is important to capture and separate ethanol from acetonitrile to use acetonitrile as the chemical feedback.[5−8] In industry, acetonitrile was purified by membrane distillation. This process is energy-intensive and inefficient because of the formation of azeotropes at a specific concentration because of the similar boiling points (acetonitrile, 81.1 °C; ethanol, 78.4 °C). Therefore, it is urgent to develop a new method for efficiently separating small molecules with similar physicochemical properties.

Recent studies have shown that porous material adsorption and separation has the advantage of high energy efficiency and low regeneration cost.[9−12] As a new generation of porous materials, coordination networks [also known as coordination polymers,[13,14] metal−organic frameworks,[15,16] or metal−organic materials (MOMs)[17,18]], have attracted much attention because of their unique porosity and chemical diversity.[19−25] In the past decades, a great number of MOMs have been already investigated for gas storage[26−28] and separations (e.g., CO_2/N_2,[29] CO_2/CH_4,[30] CO_2/CO,[31] CO_2/C_2H_2,[32,33] and C_2H_2/C_2H_4[34,35]). However, to the best of our knowledge, current MOMs did not exhibit promising liquid mixture separation, such as acetonitrile/ethanol. Thus, how to achieve efficient separation of liquid mixture (such as acetonitrile/ethanol) by MOMs is still a challenge. The naphthalene diimides containing naphthalene π-unit and imide region in forming weak supramolecular interactions are an organic electron deficient system with excellent thermal, light, and air stability.[36−41] The LUMO level of pyridine ring naphthalene diimides is −4.24 eV and the maximum absorption wavelength is 361 nm.[38] The naphthalene diimide-based coordination polymers could have abundant electronic properties that are beneficial for selective adsorption. In this study, we introduce a new coordination network constructed by a naphthalene diimide ligand, $[Cu_2(4\text{-pmntd})_2(CH_3OH)_4(opd)_2]$, which displays selective adsorp-

Received: November 20, 2018
Accepted: January 11, 2019
Published: January 25, 2019

DOI: 10.1021/acsomega.8b03229
ACS Omega 2019, 4, 1995−2000

tion water, methanol, ethanol, and separation ability of acetonitrile/ethanol.

RESULTS AND DISCUSSION

Crystal Structures and Characterizations. Solvothermal reaction of diimide-based ligand[42−44]4-pmntd and carboxyl ligand opd with $Cu(NO_3)_2{\cdot}6H_2O$ in the mixture solvents of $CHCl_3/CH_3OH/H_2O$ at 70 °C afforded green crystals of $\{[Cu_2(4\text{-pmntd})_2(CH_3OH)_4(opd)_2]\}_n$ (**1·MeOH**). Single-crystal X-ray diffraction (SCXRD) revealed that compound **1·MeOH** crystallized in orthorhombic space group *Ccca*. In **1·MeOH**, each Cu^{2+} was coordinated by two nitrogen atoms from two 4-pmntd ligands and two oxygen atoms from two opd ligands (Figure 1). It was noted that the Cu^{2+} was also

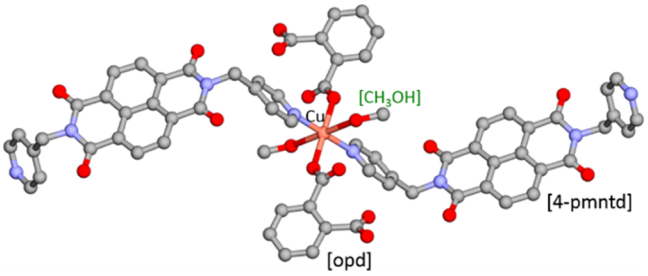

Figure 1. Coordination environments of the Cu(II) ion in compound **1·MeOH**.

bonded by two apical oxygen atoms from methanol molecules and the Cu−O bond length is 2.629 Å, indicating that there was weak interaction between Cu^{2+} and methanol molecules. Consequently, the Cu^{2+} cations of **1·MeOH** adopt an octahedral coordination geometry and serve as 4-connected nodes. The topology of this compound is a noninterpenetrated uninodal 2D network, which was revealed by the TOPOS[45] software (Figure 2). The point symbol of the framework is

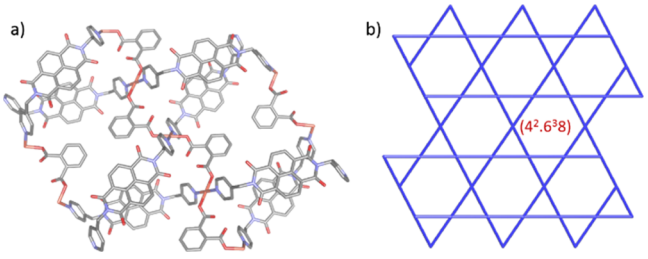

Figure 2. (a) Structure of **1·MeOH** along the *c* axis with the solvent molecules and hydrogen atoms omitted for clarity. (b) 4L1($4^2.6^3.8$) topological net.

($4^2.6^3.8$) with a 4L1 (TotUMod) topological type in the reticular chemistry structure resource.[46] The independent 2D networks are staggered relatively to each other to form rectangular-shaped tubular channels occupied by guest molecules. Thermogravimetric analysis (TGA) revealed that the as-synthesized **1·MeOH** loses guest molecules below 110 °C and retains stability until to 220 °C (Figure S3).

Compound **1·MeOH** underwent single-crystal-to-single-crystal (SCSC) transformation after the coordinated methanol molecules were removed by heating at 110 °C to form the desolvated phase, $[Cu(4\text{-pmntd})\ (opd)]_n{\cdot}$(**1·dry**). Although the crystal system and space group remain unchanged, the copper center in **1·dry** became tetra-coordinated with a quadrilateral coordination environment. Such coordination change is accompanied by apparent color change from green (**1·MeOH**) to violet (**1·dry**). Therefore, the unsaturated metal sites were formed in **1·dry** and could have potential applications for selective gas/vapor separation because of the metal−guest interactions. Interestingly, a single crystal of **1·dry** can revert to **1·MeOH** when soaked in methanol at room temperature and the color can return to green, indicating that the structural transformation is reversible. Further, **1·dry** was shown to exhibit SCSC structural change after the immersion of the single crystal into water or ethanol to form **1·H_2O** and **1·EtOH**. SCXRD revealed that the coordination geometry of Cu^{2+} in **1·H_2O** and **1·EtOH** is octahedral with coordinated solvent molecules (Figure 3).

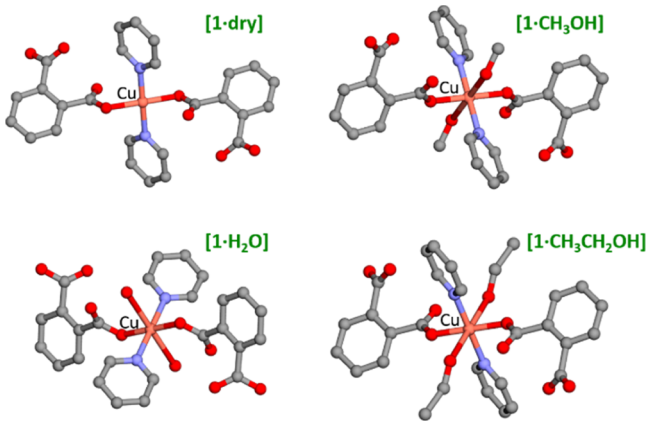

Figure 3. Single crystal structure of **1·Dry**, **1·MeOH**, **1·H_2O**, and **1·EtOH**.

Vapor Adsorption Studies. To investigate vapor sorption properties, samples of the as-synthesized **1·MeOH** were first activated to afford **1·dry** and the vapor sorption performance of **1·dry** was investigated at 298 K. For water (H_2O) adsorption, a rapid increase in the amount of adsorbed vapor under low pressure ($0 < P/P_0 < 0.02$) was observed, indicating initial adsorption with two molecules of water per unit pore. Further, at the pressure range of $0.03 < P/P_0 < 0.3$, an increase of adsorption corresponding to one molecule of water per unit pore. The third stepwise sorption was occurred at $0.3 < P/P_0 < 0.4$, revealing the adsorption of two water molecules per unit pore. H_2O adsorption reached the saturation uptake (ca. 125 $cm^3\ g^{-1}$) when the pressure over $P/P_0 > 0.4$. According to the interesting stepped isotherm, we assumed that two water molecules were first adsorbed on the unsaturated Cu^{2+} sites, followed by three water molecules entering the pores of the network. The above assumption is consistent with the results of single crystal X-ray diffraction analysis, which indicates that **1·dry** could adsorb two water molecules at the unsaturated Cu^{2+} metal site and three water molecules in the pores. Such different binding sites result in the stepped isotherm (Figure 4a). In addition, we also studied the methanol (CH_3OH) sorption of **1·dry**. Similar to water sorption, **1·dry** exhibited an initial adsorption at $0 < P/P_0 < 0.2$, which corresponding to about two methanol molecules per unit pore, and then one methanol molecule was adsorbed into the pores at $0.2 < P/P_0 < 0.8$ (Figure 4a).

Being different with water, ethanol adsorption of **1·dry** displays the one-step isotherm with uptake around 50 $cm^3\ g^{-1}$ at 100 kPa (Figure 4b). Single-crystal X-ray diffraction of **1·**

DOI: 10.1021/acsomega.8b03229
ACS Omega 2019, 4, 1995−2000

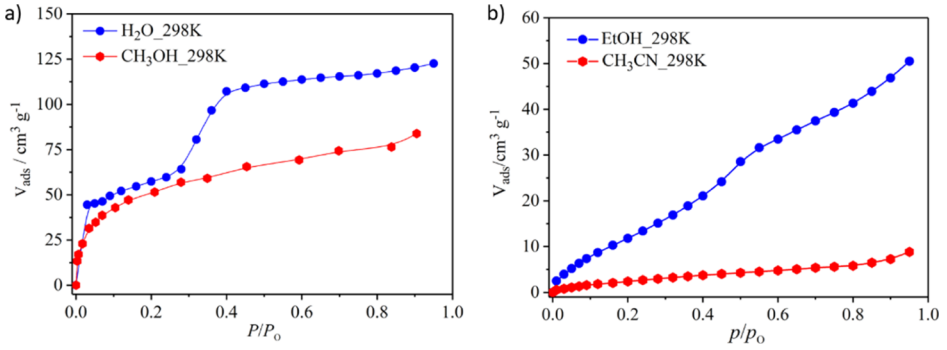

Figure 4. (a) Water and methanol adsorption isotherms of **1·dry** at 298 K. (b) Ethanol and acetonitrile absorption isotherms of **1·dry** at 298 K.

EtOH revealed that two ethanol molecules were coordinated with unsaturated Cu^{2+}. Remarkably, the acetonitrile (CH_3CN) uptake of **1·dry** at 298 K was found to be negligible (ca. 10 cm^3 g^{-1} at 100 kPa). The naphthalene diimide-based coordination polymers are hydrogen-bonded frameworks for the imide carbonyl groups being the acceptor of hydrogen-bonded. **1·dry** selective adsorption of water, methanol, and ethanol for them contain the hydroxyl groups as hydrogen-bonded donors and interact with unsaturated Cu^{2+} sites. The big molecular size and no hydroxyl group of acetonitrile can neither interact with unsaturated Cu^{2+} sites nor enter the pores (Figure 5). The

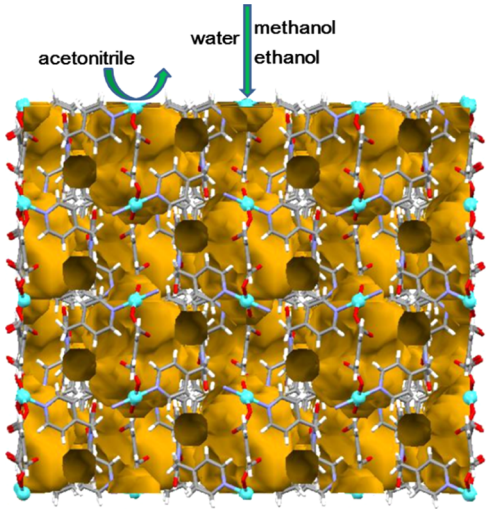

Figure 5. Schematic representation of the selective interaction between hydroxylic guests and unsaturated Cu^{2+} metal sites.

mixed solvents, ethanol and acetonitrile, are commonly used such as in phase chromatography of biomolecules and the ethanol/acetonitrile separation and recycling, which are of great significance. The high ethanol uptake and low acetonitrile uptake of **1·dry** at 100 kPa are beneficial for the ethanol/acetonitrile separation at ambient temperature.

Ethanol/Acetonitrile Separation. Given the differences in the adsorption behaviors of the **1·dry** for ethanol and acetonitrile, we utilized **1·dry** as a stationary phase to discover the separation performance of ethanol/acetonitrile binary mixtures. A column (10 × 10 × 100 mm) was packed with **1·dry** (ca. 10 g) and then let 1 mL ethanol and 1 mL acetonitrile binary mixtures pass through the column. Evolved solvent components were monitored by NMR (integrating the peak area). In the experiment, C_2H_5OH and CH_3CN were initially coadsorbed before CH_3CN was replaced by C_2H_5OH. An acetonitrile outlet purity was increased from 50 to 70% (Figure 6). We assume that the specific interaction between

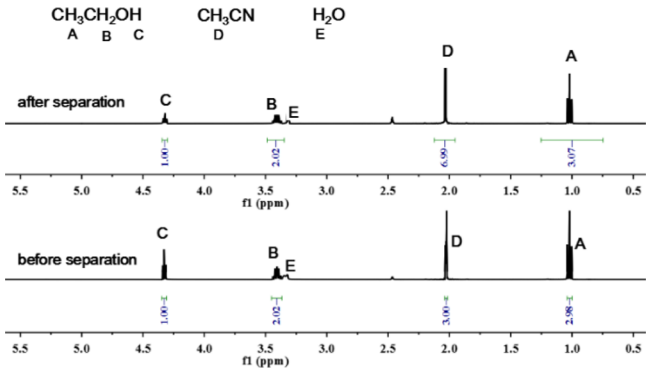

Figure 6. ^1H NMR (DMSO-d_6) spectroscopy of ethanol/acetonitrile binary mixtures before and after passing through the packed sample (**1·dry**).

unsaturated metal sites and hydroxylic guest (ethanol) plays a vital role for such real ethanol/acetonitrile separation performance. Furthermore, the TGA studies indicate that the coordinated ethanol molecules in the pores of **1·EtOH** could be removed by heating up to 110 °C and readsorbed by dispersing the material to ethanol vapor at room temperature. These procedures can be repeated for five cycles, validating the reversibility of the process (Figure S4).

CONCLUSIONS

In summary, this work demonstrates a strategy that constructed open metal sites in coordination networks and could improve the selective sorption between hydroxylic guests and nonhydroxylic guests. This new naphthalene diimide-based coordination polymer is the first example that exhibits selective separation of ethanol/acetonitrile at ambient temperature.

EXPERIMENTAL SECTION

Physical Measurements. Elemental analyses (C, H, and N) were carried out with a PerkinElmer 240C elemental analyzer. FT-IR spectra were obtained from KBr pellets in the range of 4000−400 cm^{-1} on a VECTOR 22 spectrometer. Powder X-ray diffraction (PXRD) was performed on a Bruker D8 ADVANCE diffractometer (Cu Kα, 1.5418 Å) at 40 kV and 40 mA. Thermal analyses were performed on a TGA V5.1A Dupont 2100 instrument from room temperature to

DOI: 10.1021/acsomega.8b03229
ACS Omega 2019, 4, 1995−2000

Table 1. Crystallographic Data and Structure Refinement for 1

complex	1·MeOH	1·dry	1·H_2O	1·EtOH
formula	$C_{37}H_{21}Cl_3CuN_4O_{10}$	$C_{34}H_{20}CuN_4O_{11}$	$C_{34}H_{18}CuN_4O_{14}$	$C_{38}H_{20}CuN_4O_{14}$
F_w	851.47	724.08	770.06	820.12
T (K)	150(2)	373(2)	293(2)	150(2)
wavelength (Å)	1.54178	0.71073	0.71073	1.54178
crystal system	orthorhombic	orthorhombic	orthorhombic	orthorhombic
space group	*Ccca*	*Ccca*	*Ccca*	*Ccca*
a (Å)	17.1736(6)	17.354(2)	17.033(2)	17.2256(10)
b (Å)	28.5197(11)	28.747(5)	28.521(6)	28.4486(16)
c (Å)	15.4911(5)	15.0069(19)	15.290(2)	15.7432(19)
α (deg)	90	90	90	90
β (deg)	90	90	90	90
γ (deg)	90	90	90	90
V (Å^3)	7587.3(5)	7486.4(18)	7428(2)	7714.9(11)
Z	8	8	8	8
ρ_{cal} (g cm^{-3})	1.491	1.285	1.377	1.412
μ (mm^{-1})	3.296	0.643	0.659	1.436
F (000)	3448	2952	3128	3336
reflections collected/unique	7807/2819	10305/3622	18800/3582	7019/2869
GOF	1.051	1.004	1.938	1.024
R_1, ωR_2 [$I > 2\sigma(I)$]	0.0832, 0.2568	0.0841, 0.2178	0.1284, 0.3211	0.1009, 0.2883
R_1, ωR_2 [all data]	0.0936, 0.2659	0.1937, 0.2775	0.1795, 0.3441	0.1353, 0.3315

800 °C with a heating rate of 10 °C min^{-1} in the air, and the data are consistent with the structures. The vapor adsorption isotherms (at 298 K) were measured by using the BELSORP-max automatic volumetric sorption apparatus.

General Procedures. Chemicals were purchased from commercial sources and used without further purification.

Synthesis. *{[Cu(4-pmntd)(CH_3OH)$_2$(opd)]·$CHCl_3$}$_n$(**1·MeOH**).* A mixture of 4-pmntd (6 mg, 0.0125 mmol), $Cu(NO_3)_2·6H_2O$ (8 mg, 0.025 mmol), and Na_2(opd) (21 mg, 0.1 mmol) in $H_2O/CH_3OH/CHCl_3$ (1 mL/3 mL/10 mL) was stirred and then sealed in a 20 mL Teflon-lined autoclave. The autoclave was heated to 70 °C and held at that temperature for 7 days, followed by further cooling to room temperature. Green crystals of **1** were collected in 32% yield based on the ligand. Anal. Calcd for $C_{37}H_{21}Cl_3CuN_4O_{10}$: C, 52.19; H, 2.49; N, 6.58%. Found: C, 51.85; H, 2.16; N, 6.69%. IR (KBr, cm^{-1}): 3428 vs, 1709 m, 1668 vs, 1615 m, 1580 s, 1453 w, 1429 w, 1383 s, 1336 s, 1249 m, 1179 w, 754 m, 565 w.

X-ray Crystallography. The diffraction data were collected on an Oxford Gemini S Ultra diffractometer equipped with Cu Kα radiation (λ = 1.54178 Å) for complex **1·MeOH** and **1·EtOH**, or on the same diffractometer equipped with Mo Kα radiation (λ = 0.71073 Å) for complexes **1·dry** and **1·H_2O** by using φ and ω scans. Multiscan adsorption corrections were applied for all complexes. The structures were solved by the direct methods (SHELXS) and refined by the full matrix least-squares method against F_o^2 using the SHELXTL software.[47−49] The coordinates of the nonhydrogen atoms were refined anisotropically. Most of hydrogen atoms were introduced in calculated positions and refined with a fixed geometry with respect to their carrier atoms, and the guest methanol hydrogen atoms have not been added. Details of the crystal parameters, data collections, and refinement for all compounds are summarized in Table 1. Further details are provided in the Supporting Information. CCDC numbers 966848 (**1·MeOH**), 966849 (**1·dry**), 966850 (**1·H_2O**), and 1861423 (**1·EtOH**)

■ ASSOCIATED CONTENT

Supporting Information

The Supporting Information is available free of charge on the ACS Publications website at DOI: 10.1021/acsomega.8b03229.

Two 4-pmntd structural figures, PXRD patterns, TGA, FT-IR, adsorption isotherms, tables for X-ray structural data, selected bond lengths and bond angles (PDF)
X-ray crystallographic data for (**1·MeOH**) (CIF)
X-ray crystallographic data for (**1·dry**) (CIF)
X-ray crystallographic data for (**1·H_2O**) (CIF)
X-ray crystallographic data for (**1·EtOH**) (CIF)

■ AUTHOR INFORMATION

Corresponding Author

*E-mail: qingyuan.yang@xjtu.edu.cn (Q.-Y.Y.).

ORCID

Shi-Qiang Wang: 0000-0003-1213-8317
Qing-Yuan Yang: 0000-0002-1742-2088

Notes

The authors declare no competing financial interest.

■ ACKNOWLEDGMENTS

This work was financially supported by the National Natural Science Foundation of China (no. 21403191), Natural Science Foundation of Guangdong Province (no. 2017A030307036), Special funds for public welfare research and capacity building in Guangdong Province (nos. 2015A010105031 and 2016A010103042) and Lingnan Normal University Science Research Foundation (no. LP1859). Q.-Y.Y. acknowledges the "Young Talent Support Plan" of Xi'an Jiaotong University (HG6J004).

■ REFERENCES

(1) Srinivasu, M. K.; Raju, A. N.; Reddy, G. O. Determination of lovastatin and simvastatin in pharmaceutical dosage forms by MEKC. *J. Pharm. Biomed. Anal.* **2002**, *29*, 715−721.

DOI: 10.1021/acsomega.8b03229
ACS Omega 2019, 4, 1995−2000

(2) Li, J.; Yang, X.; Chen, K.; Zheng, Y.; Peng, C.; Liu, H. Sifting Ionic Liquids as Additives for Separation of Acetonitrile and Water Azeotropic Mixture Using the COSMO-RS Method. *Ind. Eng. Chem. Res.* **2012**, *51*, 9376−9385.
(3) Rosén, J.; Hellenäs, K.-E. Analysis of acrylamide in cooked foods by liquid chromatography tandem mass spectrometry. *Analyst* **2002**, *127*, 880−882.
(4) Hu, Y.; Cao, J.; Deng, J.; Cui, B.; Tan, M.; Li, J.; Zhang, H. Synthesis of acetonitrile from ethanol via reductive amination over Cu/γ-Al2O3. *React. Kinet., Mech. Catal.* **2012**, *106*, 127−139.
(5) Brettschneider, F.; Jankowski, V.; Günthner, T.; Salem, S.; Nierhaus, M.; Schulz, A.; Zidek, W.; Jankowski, J. Replacement of acetonitrile by ethanol as solvent in reversed phase chromatography of biomolecules. *J. Chromatogr. B: Anal. Technol. Biomed. Life Sci.* **2010**, *878*, 763−768.
(6) Khayet, M.; Cojocaru, C.; Zakrzewska-Trznadel, G. Studies on pervaporation separation of acetone, acetonitrile and ethanol from aqueous solutions. *Sep. Purif. Technol.* **2008**, *63*, 303−310.
(7) Yang, S.; Wang, Y.; Bai, G.; Zhu, Y. Design and Control of an Extractive Distillation System for Benzene/Acetonitrile Separation Using Dimethyl Sulfoxide as an Entrainer. *Ind. Eng. Chem. Res.* **2013**, *52*, 13102−13112.
(8) Li, J. D.; Wang, M. M.; Huang, Y. C.; Luo, B. B.; Zhang, Y.; Yuan, Q. Separation of Binary Solvent Mixtures with Solvent Resistant Nanofiltration Membranes Part A: Investigation of Separation Performance. *RSC Adv.* **2014**, *4*, 40740.
(9) Li, J.-R.; Sculley, J.; Zhou, H.-C. Metal−organic frameworks for separations. *Chem. Rev.* **2011**, *112*, 869−932.
(10) Van de Voorde, B.; Bueken, B.; Denayer, J.; De Vos, D. Adsorptive separation on metal−organic frameworks in the liquid phase. *Chem. Soc. Rev.* **2014**, *43*, 5766−5788.
(11) Lozano-Castelló, D.; Alcañiz-Monge, J.; de la Casa-Lillo, M. A.; Cazorla-Amorós, D.; Linares-Solano, A. Advances in the study of methane storage in porous carbonaceous materials. *Fuel* **2002**, *81*, 1777−1803.
(12) Menon, V. C.; Komarneni, S. Porous Adsorbents for Vehicular Natural Gas Storage: A Review. *J. Porous Mater.* **1998**, *5*, 43−58.
(13) Kitagawa, S.; Kitaura, R.; Noro, S.-i. Functional Porous Coordination Polymers. *Angew. Chem., Int. Ed.* **2004**, *43*, 2334−2375.
(14) Batten, S. R.; Neville, S. M.; Turner, D. R. *Coordination Polymers:Design, Analysis and Application Introduction*; RSC Publishing: Cambridge, 2009.
(15) Furukawa, H.; Cordova, K. E.; O'Keeffe, M.; Yaghi, O. M. The chemistry and applications of metal-organic frameworks. *Science* **2013**, *341*, 1230444.
(16) MacGillivray, L. R. *Metal-Organic Frameworks:Design and Application*; Wiley: Hoboken, 2010.
(17) Perry, J. J.; Perman, J. A.; Zaworotko, M. J. Design and synthesis of metal−organic frameworks using metal−organic polyhedra as supermolecular building blocks. *Chem. Soc. Rev.* **2009**, *38*, 1400−1417.
(18) Cook, T. R.; Zheng, Y.-R.; Stang, P. J. Metal−Organic Frameworks and Self-Assembled Supramolecular Coordination Complexes: Comparing and Contrasting the Design, Synthesis, and Functionality of Metal−Organic Materials. *Chem. Rev.* **2012**, *113*, 734−777.
(19) Moulton, B.; Zaworotko, M. J. From Molecules to Crystal Engineering: Supramolecular Isomerism and Polymorphism in Network Solids. *Chem. Rev.* **2001**, *101*, 1629−1658.
(20) Yang, Q.-Y.; Chen, K.-J.; Schoedel, A.; Wojtas, L.; Perry, J. J., IV; Zaworotko, M. J. Network diversity through two-step crystal engineering of a decorated 6-connected primary molecular building block. *CrystEngComm* **2016**, *18*, 8578−8581.
(21) Stock, N.; Biswas, S. Synthesis of Metal-Organic Frameworks (MOFs): Routes to Various MOF Topologies, Morphologies, and Composites. *Chem. Rev.* **2011**, *112*, 933−969.
(22) Yang, Q.-Y.; Pan, M.; Wei, S.-C.; Li, K.; Du, B.-B.; Su, C.-Y. Linear Dependence of Photoluminescence in Mixed Ln-MOFs for Color Tunability and Barcode Application. *Inorg. Chem.* **2015**, *54*, 5707−5716.
(23) Zhang, J. P.; Zhou, H. L.; Zhou, D. D.; Liao, P. Q.; Chen, X. M. Controlling flexibility of metal−organic frameworks. *Natl. Sci. Rev.* **2017**, *5*, 907.
(24) Wang, S.-Q.; Yang, Q.-Y.; Mukherjee, S.; O'Nolan, D.; Patyk-Kaźmierczak, E.; Chen, K.-J.; Shivanna, M.; Murray, C.; Tang, C. C.; Zaworotko, M. J. Recyclable switching between nonporous and porous phases of a square lattice (sql) topology coordination network. *Chem. Commun.* **2018**, *54*, 7042−7045.
(25) Shivanna, M.; Yang, Q. Y.; Bajpai, A.; Sen, S.; Hosono, N.; Kusaka, S.; Pham, T.; Forrest, K. A.; Space, B.; Kitagawa, S.; Zaworotko, M. J. Readily accessible shape-memory effect in a porous interpenetrated coordination network. *Sci. Adv.* **2018**, *4*, eaaq1636.
(26) He, Y.; Zhou, W.; Qian, G.; Chen, B. Methane storage in metal−organic frameworks. *Chem. Soc. Rev.* **2014**, *43*, 5657−5678.
(27) Yang, Q.-Y.; Lama, P.; Sen, S.; Lusi, M.; Chen, K.-J.; Gao, W.-Y.; Shivanna, M.; Pham, T.; Hosono, N.; Kusaka, S.; Perry, J. J.; Ma, S.; Space, B.; Barbour, L. J.; Kitagawa, S.; Zaworotko, M. J. Reversible Switching between Highly Porous and Nonporous Phases of an Interpenetrated Diamondoid Coordination Network That Exhibits Gate-Opening at Methane Storage Pressures. *Angew. Chem., Int. Ed.* **2018**, *57*, 5684−5689.
(28) Peng, Y.; Krungleviciute, V.; Eryazici, I.; Hupp, J. T.; Farha, O. K.; Yildirim, T. Methane Storage in Metal−Organic Frameworks: Current Records, Surprise Findings, and Challenges. *J. Am. Chem. Soc.* **2013**, *135*, 11887−11894.
(29) Nugent, P.; Belmabkhout, Y.; Burd, S. D.; Cairns, A. J.; Luebke, R.; Forrest, K.; Pham, T.; Ma, S.; Space, B.; Wojtas, L.; Eddaoudi, M.; Zaworotko, M. J. Porous materials with optimal adsorption thermodynamics and kinetics for CO_2 separation. *Nature* **2013**, *495*, 80−84.
(30) Taylor, M. K.; Runčevski, T.; Oktawiec, J.; Bachman, J. E.; Siegelman, R. L.; Jiang, H.; Mason, J. A.; Tarver, J. D.; Long, J. R. -Perfect CO_2/CH_4 Selectivity Achieved through Reversible Guest Templating in the Flexible Metal−Organic Framework Co(bdp). *J. Am. Chem. Soc.* **2018**, *140*, 10324−10331.
(31) Long, K.-J.; Yang, Q.-Y.; Sen, S.; Madden, D. G.; Kumar, A.; Pham, T.; Forrest, K. A.; Hosono, N.; Space, B.; Kitagawa, S.; Zaworotko, M. J. Efficient CO_2 Removal for Ultra-Pure CO Production by Two Hybrid Ultramicroporous Materials. *Angew. Chem., Int. Ed.* **2018**, *57*, 3332−3336.
(32) Chen, K.-J.; Scott, H. S.; Madden, D. G.; Pham, T.; Kumar, A.; Bajpai, A.; Lusi, M.; Forrest, K. A.; Space, B.; Perry, J. J.; Zaworotko, M. J. Benchmark C_2H_2/CO_2 and CO_2/C_2H_2 Separation by Two Closely Related Hybrid Ultramicroporous Materials. *Chem* **2016**, *1*, 753−765.
(33) Luo, F.; Yan, C.; Dang, L.; Krishna, R.; Zhou, W.; Wu, H.; Dong, X.; Han, Y.; Hu, T.-L.; O'Keeffe, M.; Wang, L.; Luo, M.; Lin, R.-B.; Chen, B. UTSA-74: A MOF-74 Isomer with Two Accessible Binding Sites per Metal Center for Highly Selective Gas Separation. *J. Am. Chem. Soc.* **2016**, *138*, 5678−5684.
(34) Cui, X.; Chen, K.; Xing, H.; Yang, Q.; Krishna, R.; Bao, Z.; Wu, H.; Zhou, W.; Dong, X.; Han, Y.; Li, B.; Ren, Q.; Zaworotko, M. J.; Chen, B. Pore chemistry and size control in hybrid porous materials for acetylene capture from ethylene. *Science* **2016**, *353*, 141−144.
(35) Hu, T. L.; Wang, H.; Li, B.; Krishna, R.; Wu, H.; Zhou, W.; Zhao, Y.; Han, Y.; Wang, X.; Zhu, W.; Yao, Z.; Xiang, S.; Chen, B. Microporous metal−organic framework with dual functionalities for highly efficient removal of acetylene from ethylene/acetylene mixtures. *Nat. Commun.* **2015**, *6*, 7328−7336.
(36) Ajayakumar, M. R.; Mukhopadhyay, P. Naphthalene-bis-hydrazimide: radical anions and ICT as new bimodal probes for differential sensing of a library of amines. *Chem. Commun.* **2009**, 3702−3704.
(37) Kumar, Y.; Kumar, S.; Mandal, K.; Mukhopadhyay, P. Isolation of Tetracyano-Naphthalenediimide and its Ambient Stable Planar Radical Anion. *Angew. Chem., Int. Ed.* **2018**, *57*, 16318−16322.

DOI: 10.1021/acsomega.8b03229
ACS Omega 2019, 4, 1995−2000

(38) Kumar, S.; Shukla, J.; Kumar, Y.; Mukhopadhyay, P. Electron-Poor Arylenediimides. *Org. Chem. Front.* **2018**, *5*, 2254−2276.
(39) Kumar, S.; Mukhopadhyay, P. Ambient Stable Naphthalene-diimide Radical Ions: Synthesis by Solvent-Free, Sonication, Mechanical Grinding or Milling Protocols. *Green Chem.* **2018**, *20*, 4620−4628.
(40) Sakai, N.; Mareda, J.; Vauthey, E.; Matile, S. Core-substituted naphthalenediimides. *Chem. Commun.* **2010**, *46*, 4225−4237.
(41) Suraru, S.-L.; Würthner, F. Strategies for the Synthesis of Functional Naphthalene Diimides. *Angew. Chem., Int. Ed.* **2014**, *53*, 7428−7448.
(42) Li, G.-B.; Liao, Z.-H.; Pan, R.-K.; Liu, J.-M.; Liu, S.-G.; Zhang, Z. Synthesis, fluorescence, and sorption properties of cobalt coordination polymers of the N,N'-bis(4-pyridylmethyl)naphthalene diimide ligand. *Transition Met. Chem.* **2015**, *40*, 691−697.
(43) Li, G.-B.; Yang, Q.-Y.; Pan, R.-K.; Liu, S.-G. Diverse cobalt(II) coordination polymers for water/ethanol separation and luminescence for water sensing applications. *CrystEngComm* **2018**, *20*, 3891−3897.
(44) Li, G.-B.; He, J.-R.; Pan, M.; Deng, H.-Y.; Liu, J.-M.; Su, C.-Y. Construction of 0D to 3D cadmium complexes from different pyridyl diimide ligands. *Dalton Trans.* **2012**, *41*, 4626−4633.
(45) Blatov, V. A.; Shevchenko, A. P.; Proserpio, D. M. Applied Topological Analysis of Crystal Structures with the Program Package ToposPro. *Cryst. Growth Des.* **2014**, *14*, 3576−3586.
(46) O'Keeffe, M.; Peskov, M. A.; Ramsden, S. J.; Yaghi, O. M. The Reticular Chemistry Structure Resource (RCSR) Database of, and Symbols for, Crystal Nets. *Acc. Chem. Res.* **2008**, *41*, 1782−1789.
(47) Sheldrick, G. M. *SHELXS-97, Program for the Solution of Crystal Structures*; University of Göttingen: Germany, 1997.
(48) Sheldrick, G. M. *SHELXL-97, Program for the Refinement of Crystal Structures from Diffraction Data*; University of Göttingen: Göttingen (Germany), 1997.
(49) CCDC numbers: 966848 (1·MeOH), 966849 (1·dry), 966850 (1·H2O) and 1861423 (1·EtOH).

DOI: 10.1021/acsomega.8b03229
ACS Omega 2019, 4, 1995−2000